

Seasonal storage for space heating using solar DHW surplus

Gonçalo J. Brites^{*}, Manuel Garruço, Marco S. Fernandes, Diogo M. Sá Pinto, Adélio R. Gaspar

Univ Coimbra, ADAI, Department of Mechanical Engineering, Rua Luís Reis Santos, Pólo II, 3030-788, Coimbra, Portugal

ARTICLE INFO

Keywords:

Solar energy
Seasonal thermal energy storage
Sensible heat storage
DHW
Space heating
Contents

ABSTRACT

Due to the seasonality of solar energy, achieving 100 % of annual solar fraction for domestic hot water (DHW) production is only possible by greatly oversizing the collector area of a solar system, thus creating a significant energy surplus in summer. This simulation study investigates the possibility of using this surplus to promote space heating during winter, in a moderate South European climate, to try achieving a total solar fraction of 100 %. Priority is given to the DHW reservoir, diverting the excess heat to an additional large-capacity seasonal thermal energy storage (STES) reservoir. The best configuration for the number of collectors and STES tank volume was assessed through a parametric study, to reach a compromise between a high solar fraction and a reasonable system efficiency. The results showed that a system with 10 m² of solar collectors and a 30 m³ STES tank or, alternatively, 20 m² of collectors and a 20 m³ tank achieved the desired solar fraction and efficiency for the chosen building and local climate conditions. A comparison with the literature shows that this strategy can achieve better results, requiring less collector area and storage volume.

1. Introduction

In the last century, the abundance of fossil allowed for unprecedented technological, economic, and social progress in human history. However, its overuse is now prompting severe environmental problems. The result of burning fuels and the release of other anthropogenic greenhouse gas (GHG) emissions have altered the thermal balance of the planet, increasing the greenhouse effect and leading to global warming [1]. To counteract climate change, it is urgent to reduce fossil fuel use, improve energy efficiency, and increase the use of renewable energy sources. Solar energy, a clean and very accessible resource, can generate both electricity and heat without releasing GHG emissions. Despite its intermittent nature, if combined with proper storage, it provides a sustainable solution, reducing fuel combustion and optimizing energy utilization [2].

Seasonal Thermal Energy Storage (STES) systems for Space Heating (SH) and Domestic Hot Water (DHW) capture and store energy from a sustainable source, to be used later when the energy needs increase, thus dealing with the mismatch between the heat supply and demand [3,4]. The solar energy's intermittent nature makes solar thermal systems very interesting to explore in this context, with the excess energy in the summer (when the needs are lower) being stored for use in winter (when the demand is higher than the supply) [5]. In recent years, several studies [5–8] have been conducted to minimize backup energy

consumption (and therefore decrease the carbon footprint), increase the solar fraction, as well as the overall efficiency and energy density of solar thermal systems employing STES.

STES systems can be generally classified into Sensible Heat Storage (SHS) systems, Latent Heat Storage (LHS) systems and Thermochemical Heat Storage (THS) systems. Pinel et al. [6] presents an extended discussion on the methods for STES focusing on the residential scale, while Xu et al. [5] describe the different types and materials available for large STES systems. SHS is cost-effective and reliable but requires large volumes and insulation [5]. To overcome the low energy storage density, LHS and THS (sorption and chemical) are being currently investigated. LHS is based on the phase change enthalpy of a material between the liquid and solid states. It offers high heat exchange at constant temperatures but lacks suitable natural materials, leading to reliance on costly synthetics. THS, including sorption and chemical storage, is based in a reaction between two materials. It boasts high energy density and long-term storage without loss, yet is limited by material suitability and system integrity under non-atmospheric pressure [9,10]. And while there are some prototypes of sorption storage systems, chemical storage is still in development [5].

SHS systems are the most widespread and mature technology for energy storage, first started being researched in the 1940s to provide thermal energy to multiple residences [6]. It gained significant interest in the 1980s across Europe, notably in countries of higher latitude, with Sweden leading the construction of solar thermal plants with seasonal

^{*} Corresponding author. Department of Mechanical Engineering, Rua Luís Reis Santos, Pólo II, 3030-788, Coimbra, Portugal.

E-mail address: goncalo.brites@uc.pt (G.J. Brites).

<https://doi.org/10.1016/j.renene.2024.120889>

Received 1 January 2024; Received in revised form 23 May 2024; Accepted 27 June 2024

Available online 28 June 2024

0960-1481/© 2024 The Authors. Published by Elsevier Ltd. This is an open access article under the CC BY license (<http://creativecommons.org/licenses/by/4.0/>).

Nomenclature	
c_w	Specific heat of liquid water, in $\text{kJ}/(\text{kg}\cdot\text{K})$
dt	Time interval, in s or h
e	Thickness, in m or mm
f_{solar}	Solar fraction
$g_{\perp, \text{glass}}$	Solar transmission factor for an incidence of solar radiation perpendicular to the glass
\bar{H}	Daily global horizontal radiation (monthly average), in MJ/m^2 or kWh/m^2
$I_{\text{solar, col}}$	Total solar radiation incident on the collector plane per unit area, in MJ/m^2 or kWh/m^2
\dot{m}	Mass flow rate, in kg/s
Q	Heating energy, in kJ or MJ
t	Time, in s or h
T	Temperature, in $^{\circ}\text{C}$ or K
U	Heat transfer coefficient, in $\text{W}/(\text{m}^2\cdot\text{K})$
Greek Letters	
ΔT	Temperature difference, in $^{\circ}\text{C}$
η	Efficiency
λ	Thermal conductivity, in $\text{W}/(\text{m}\cdot^{\circ}\text{C})$
Subscripts	
col	(Solar) collectors
cw	Cold water
hw	Hot water
in	Inlet
out	Outlet
RF	Radiant Floor
Acronyms	
ACH	Air Changes per Hour
DHW	Domestic Hot Water
EPS	Expanded Polystyrene
HDD	Heating Degree Days
LHS	Latent Heat Storage
PID	Proportional Integral Derivative (Controller)
SH	Space Heating
SHS	Sensible Heat Storage
STES	Seasonal Thermal Energy Storage
THS	Thermochemical Heat Storage

storage. More recently, a central solar heating plant with seasonal storage to serve 500 dwellings in Zaragoza, Spain was assessed in Ref. [11]. Another study, in Australia, showed that combining solar heat for DHW and Space Heating with seasonal storage was both technically and economically viable [12], with Sydney and Perth achieving solar fractions of near 100 %. Research also highlights STES's adaptability in smart energy systems at the district level [13].

STES systems are more cost-effective at community scale, with 30 installations built in the 1980s for district heating [14]. Single housing is still prevalent, as such, several small-scale, decentralised systems have also been studied in recent years [5]. Kroll and Ziegler [15] demonstrated that small STES systems can achieve the same levels of efficiency of community-scale installations if correctly designed, with heat storage ranging from 30 to 270 kWh/m^3 , while large systems have an annual useful heat between 20 and 170 kWh/m^3 . STES systems can be used as part of passive design strategies, as evidenced in Refs. [16,17], which developed a solar thermal system in Ireland by employing evacuated tube collectors and a STES tank in a passive house, achieving 56 % of solar fraction for space heating and 93 % for DHW. Further research [18] simulated a high-efficiency STES with a large, insulated tank and evacuated tube collectors, to overcome the annual energy needs of a 150 m^2 house, achieving a 98 % solar fraction under ideal conditions. Subsequent work [19] implemented a water-to-water heat pump, increasing the solar fraction up by 2 % due to a higher storage efficiency. A Carleton University (Ottawa, Canada) study [20] confirmed the system's effectiveness in a real-world setting. A solar fraction of 64 % was achieved for both DHW and Space Heating, with the overall efficiency of the seasonal storage system reaching 42 %.

Multifamily residences also benefit from STES, as shown by a Swiss study [7] with a 180 m^3 reservoir and flat plate collectors, ensuring full solar heating to a 924 m^2 heated floor building. In the UK, the viability of STES using solar energy in the residential sector was confirmed across eight different cities, with different heat demands of space and hot water and distinct heat loss coefficients [21]. A subsequent study [22] considered an ammonia-based chemisorption STES, achieving 57 % of space heating demand. A study in Thessaloniki, Greece simulated a solar thermal system with seasonal storage for homes using TRNSYS [23]. A 120 m^2 home used two tanks, one for daily DHW use and another with seasonal storage for space heating purposes, achieving 52 % heating efficiency, later optimized to 67 % [24].

LHS and THS systems, though less disseminated and explored, show

promise. A lab-scale system with sodium acetate trihydrate for energy storage achieved promise results for domestic dwellings in the Danish climate [25]. A Turkish system used paraffin wax to heat a 180 m^2 greenhouse, achieving a 74 % efficiency [26]. Another study highlighted an adsorption system with an 84 % solar fraction and a 178 kWh/m^3 energy density for home heating [27].

The literature suggests that for small residential buildings sensible using large water tanks is still the most feasible option. However, studies are still limited, focusing mainly on colder climates, with large solar STES systems that are not able to fully meet both DHW and space heating demands. In warmer locations, the focus is mainly on DHW, with less need for space heating. In Portugal, residential buildings' energy demand for heating, cooling and DHW is influenced by the mild climate, which dictates less energy for heating compared to colder European countries. The technology mix includes both traditional systems and renewable energy sources, with solar thermal technology increasingly used for DHW. National regulations, aligned with EU directives, aim to improve energy efficiency, particularly in the older housing stock. However, the rate of energy-saving retrofitting is low, and there is a push towards increasing renewable energy usage, especially solar, to reduce reliance on fossil fuels and enhance overall energy efficiency in the residential sector [28–30]. In addition, the potential for district heating and cooling networks is very low or almost non-existent in Portugal [31]. In this context, giving that the solar energy available in summer usually surpasses the DHW requirements, it would make sense to make use of this surplus energy to help meeting the space heating demands during the heating season.

The objective of this work is thus to design and assess a solar STES system able to fully meet the annual DHW demand of a single-family house located in Portugal, while making use of the surplus solar energy in summer to also meet the space heating demand during winter. The priority is given to DHW due its higher temperature needs comparing to radiant space heating. The DHW tank size matches the DHW demand, being then necessary to assess the area of the solar collector field and the STES tank volume. For this purpose, a parametric study is carried out, since the best compromise between a high solar fraction and a reasonable overall efficiency or an acceptable total system cost requires a proper evaluation of the parameters evolution and not an optimization analysis, which could lead to inadequate results (e.g., too large oversizing to reach 100 % solar fraction, or too low solar fraction if the goal is to reduce costs). The impact of the system size on its efficiency

and cost is to be evaluated in detail, and the results to be compared with similar research works, trying to evaluate the application of such system in the Portuguese climate.

2. Materials and methods

For the purpose of this study, an idealized model of a building with a thermal envelope well adapted to the local climate and with typical occupation and internal gains was considered. The type of building selected was a single-story detached house, and care was taken to follow the national regulations regarding room and window sizes and construction heat transfer coefficients. The dwelling comprises a solar thermal system for DHW and underfloor heating, with seasonal storage. The building and its systems were modeled using TRNSYS 18.

2.1. Location

The chosen location is Coimbra, Portugal (latitude 40.20 N, longitude 8.41 W, and altitude 141 m), for which the correspondent TRNSYS weather file was used (TMY2 data).

Coimbra has a warm-summer Mediterranean climate (Csb, according to the Köppen-Geiger classification [32]) in a transition to a hot-summer (Csa) version of the interior of Central Portugal, with mild, relatively rainy winters. As can be seen in Fig. 1, there are four distinct seasons. In winter, the monthly average daily global horizontal radiation, \bar{H} , reaches a minimum of 6 MJ/m², the temperatures range between 15 and 16 °C during the day and 5–7 °C at night, and occasionally the temperature can drop below 0 °C (around 10 days during the year). In summer, \bar{H} can reach 24 MJ/m², and the temperatures range between 28 and 29 °C during the day and 15–16 °C at night, but on the hottest days it can reach 40 °C or more. In spring and autumn, the solar radiation and temperature present intermediate values.

2.2. Building specifications

The building is a single-story detached house with an area of 115 m² and a ceiling height of 2.7 m, whose plan is represented in Fig. 2. The building was modeled in detail, i.e., each space in the plan corresponds to a single thermal zone in the model. It comprises a kitchen + living room in the central section, three bedrooms, an office, and two bathrooms.

The geometric model of the house was developed with the TRNSYS Plugin for Sketchup 2017 and can be seen in Fig. 3. The composition of the walls, floors, ceilings, and roof, as well as windows and doors, was chosen according to the most common practice in the region. Table 1 presents the materials of the layers for each construction and the

corresponding heat transfer coefficient. The attic has no lighting or equipment heat gains, and it can be considered a strongly ventilated space.

An external shading of the windows was implemented in the model. The window panes are shaded during the cooling season (between May and October) with exterior shutters to avoid overheating, but shading is disabled in the winter months to increase the internal solar gains and reduce heating loads.

The building is ventilated by infiltration only. Given the uncertainty in the air infiltration calculations, a constant value of 0.4 air changes per hour (ACH) was considered in all occupied spaces. In the attic, which is supposed to be strongly ventilated, a constant value of 2 ACH was defined.

An occupation of four people was considered, and typical internal loads (occupation, lighting, and equipment) were defined, based on average energy and DHW consumption of a Portuguese family, according to data published by PORDATA [33] and by INE and DGEG [34]. DHW consumption was adapted from the standard consumption defined by the Portuguese energy certification legislation: for each day, and for one person, the typical DHW consumption is 0.04 m³ at 50 °C. In the model, the DHW consumption is considered at a temperature of 45 °C. Using the equivalence stated in eq. (1), the total daily DHW consumption considered is 0.18 m³ at 45 °C.

$$m_1 c_w \Delta T_1 = m_2 c_w \Delta T_2 \quad (1)$$

The DHW profile considered for this case considers higher DHW needs early in the morning, and later at the end of the day. The profile is represented in Fig. 4.

2.3. Solar thermal system with DHW and STES

The schematic diagram of the solar thermal system with DHW, STES, and underfloor heating is represented in Fig. 5. The number of solar thermal collectors is deliberately oversized to reach an annual DHW solar fraction near 100 %, resulting in a large surplus of thermal energy production during the summer season, which will be stored for heating the house during the winter. The DHW storage tank meets the daily hot water needs (short-term storage) and the large STES tank with a very thick insulation layer stores the surplus heat produced during the summer (long-term storage) and supplies thermal energy to the radiant floor heating system during the winter.

The control system gives priority to DHW production whenever the DHW reservoir is at a temperature below 60 °C. When it reaches 65 °C, valve 1 directs the thermal fluid to the STES reservoir. A 5 °C deadband is set to provide control stability. Valve 4 is a thermostatic mixing valve to prevent scalding and valve 5 is a bypass valve to limit the inlet

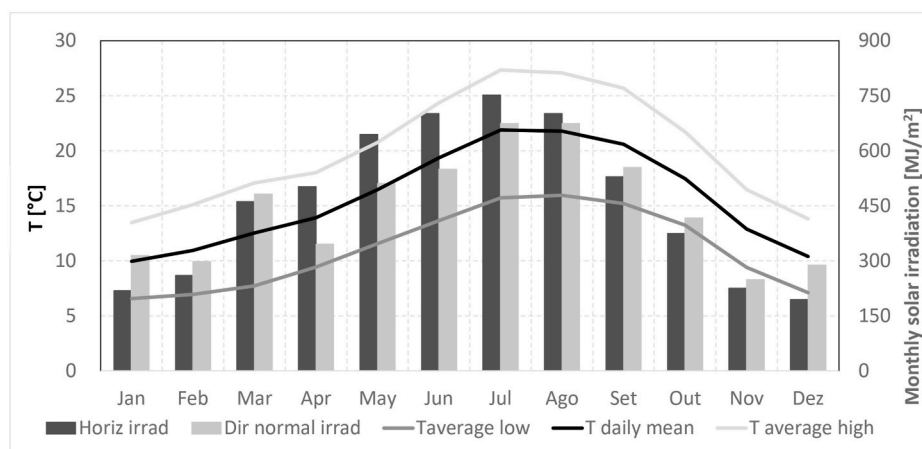


Fig. 1. Monthly variation of solar radiation and air temperature in Coimbra. Data extracted from TRNSYS TMY2 weather file.

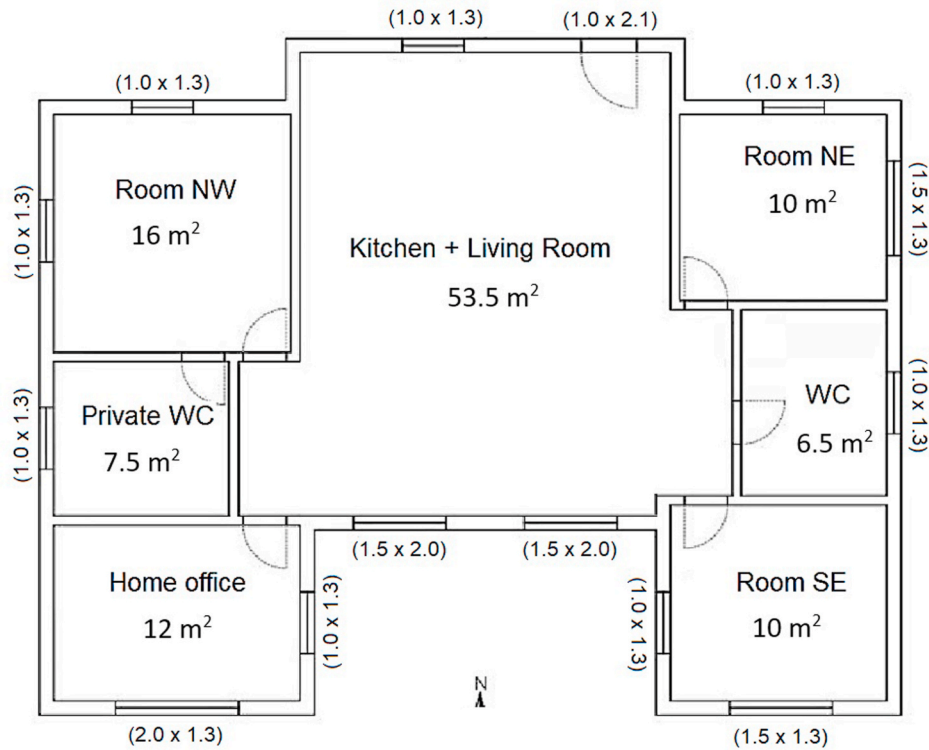


Fig. 2. Plan of the house with spaces and areas.

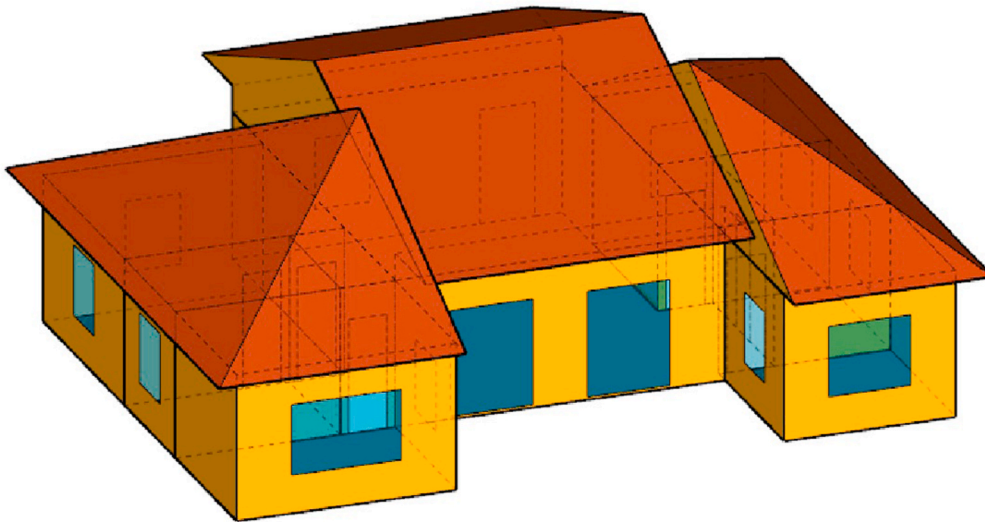


Fig. 3. Sketchup model of the house seen in perspective.

temperature of the underfloor heating system.

Both the domestic hot water and the underfloor heating have an instantaneous heating system (backup heating) that only switches on when the water or thermal fluid is below the defined setpoints (45 °C for DHW and 30 °C for the radiant floor heating). For the purposes of this study, a generic backup heating system was considered, as only the total backup energy required is relevant for the analysis.

The DHW reservoir is a 1.5 m high cylindrical tank, with 0.18 m³ internal volume and 60 mm thick EPS thermal insulation. The STES tank is also a cylindrical tank made of fiber-reinforced plastic, with 1.8 m high and 400 mm thick EPS thermal insulation, buried 1 m below the surface. The optimal insulation thickness values were studied in

Ref. [35]. The tank volume will be a result of the present study. Both tanks present thermal stratification, calculated with 10 nodes. The inlets and outlets are located in the bottom and upper nodes, respectively. The heat input is transferred to the tank via an internal coiled tube exchanger.

The solar collectors are flat plate collectors with 2.09 m² aperture area and coefficients $a_0 = 0.684$, $a_1 = 3.64 \text{ W/m}^{-2}\cdot\text{K}^{-1}$ and $a_2 = 0.012 \text{ W/m}^{-2}\cdot\text{K}^{-2}$. They are oriented towards the south with an inclination angle of 45°. This value resulted from a parametric study, presented in Ref. [35], in which the collector's tilt was varied between 35° and 60°, in intervals of 5°, with the minimum auxiliary energy value occurring at 45°. The number of collectors will be a result of the present study.

Table 1

Composition of the walls, floors, ceilings, windows, and doors, the properties of materials, and the corresponding heat transfer coefficient.

Type of construction	Materials	U [W·m ⁻² ·K ⁻¹]
External walls	Plaster (external surface layer, e = 0.02 m; λ = 1.3 W/(m·K)) EPS (thermal insulation, e = 0.07 m; λ = 0.037 W/(m·K)) Clay bricks (hollow, e = 0.15 m; λ = 0.38 W/(m·K)) Plaster (internal surface layer, e = 0.02 m; λ = 1.3 W/(m·K))	0.402
Ceiling slab	XPS (external surface layer, thermal insulation, e = 0.09 m; λ = 0.037 W/(m·K)) Lightened slab (joists and hollow clay bricks, e = 0.33 m; λ = 1.05 W/(m·K)) Plaster (internal surface layer, e = 0.02 m; λ = 1.3 W/(m·K))	0.340
Floor slab	Gravel rock bed (contact with the ground, e = 0.1 m; λ = 2.0 W/(m·K)) Concrete slab (steel reinforced, e = 0.2 m; λ = 2.0 W/(m·K)) XPS (thermal insulation, e = 0.03 m; λ = 0.037 W/(m·K)) Leveling screed (contains the radiant floor pipes, e = 0.06 m; λ = 1.3 W/(m·K)) Mortar (e = 0.015 m; λ = 1.3 W/(m·K)) Ceramic tile (internal layer, e = 0.01 m; λ = 1.3 W/(m·K))	0.805
Windows/ external doors	Double glass pane (aluminum frame, g _{l, glass} = 0.7) All windows have an external shading device	2.430
Internal partitions	Plaster (internal surface layer, e = 0.02 m; λ = 1.3 W/(m·K)) Clay bricks (hollow, e = 0.11 m; λ = 0.41 W/(m·K)) Plaster (internal surface layer, e = 0.02 m; λ = 1.3 W/(m·K))	1.790
Internal doors	Medium density fiberboard – MDF (e = 0.03 m; λ = 0.14 W/(m·K))	2.110

2.4. Simulation model

Fig. 6 displays a simplified layout of the TRNSYS model. On top there is the building object (TRNSYS type 56) and the meteorological data file reader (type 15-6). Below the building there is a set of PID controls (type 23), comprising the controls for each room with underfloor heating, acting on the flow passing through the radiant floor pipes to maintain the setpoint temperature. A bypass (type 115) between the radiant floor

manifolds (types 647, 649) prevents space overheating and waste of thermal energy. The tee (type 11h) before the pump (type 114) mixes the hot stream from the STES tank (type 1534-coiled) with part of the return flow to keep the supply temperature at a constant value of 30 °C. An auxiliary heater (type 138) heats the mixed flow whenever the temperature drops below the setpoint.

The control of the solar collector loop operates according to the block diagram in Fig. 7. It turns the solar pump on only if the temperature of the solar collectors (type 1346) is higher than at least one of the storage tank temperatures. If the temperature of the solar collectors is higher than the DHW storage temperature, the controller gives priority to the DHW tank (type 1534-coiled), but when this tank temperature reaches 65 °C the flow is diverted (diverter type 11f) to the STES tank, which exchanges heat with the soil (type 1302). No energy from STES can be used in DHW production, since the system prioritizes DHW, and only excess heat is stored in STES reservoir. The DHW consumption profile (type 14h) is displayed at the bottom. A diverter controlled by the DHW tank's temperature (type 11b) and an auxiliary heater (type 138) guarantee the temperature of 45 °C for DHW consumption.

Since the simulation is ran with an initial guess value for the STES tank temperature, a test was carried out by repeating the simulation for several consecutive years to obtain reliable results. The annual values of the system components' energy balances (solar loop, STES storage, radiant floor, etc), were checked for each year to determine when the results stabilize, taking 4 consecutive simulated years for that to take place. Therefore, for all tested cases, 4 consecutive years, with a time-step of 6 min, are simulated and only the results of the last year are considered valid.

2.5. Metrics

The building has thermal needs for domestic hot water (DHW) and space heating (SH). Water for SH circulates through the radiant floor pipes to meet the thermal loads of the occupied spaces, maintaining an indoor air temperature of at least 20 °C from November to April (heating season). The thermal energy supplied to the DHW in a certain period is calculated as:

$$Q_{DHW} = \int_0^t \dot{m}_{DHW} \cdot c_w \cdot (T_{hw} - T_{cw}) \cdot dt \quad (2)$$

While the thermal energy supplied to the SH water can be calculated as follows:

$$Q_{SH} = \int_0^t \dot{m}_{SH} \cdot c_w \cdot (T_{RF,in} - T_{RF,out}) \cdot dt \quad (3)$$

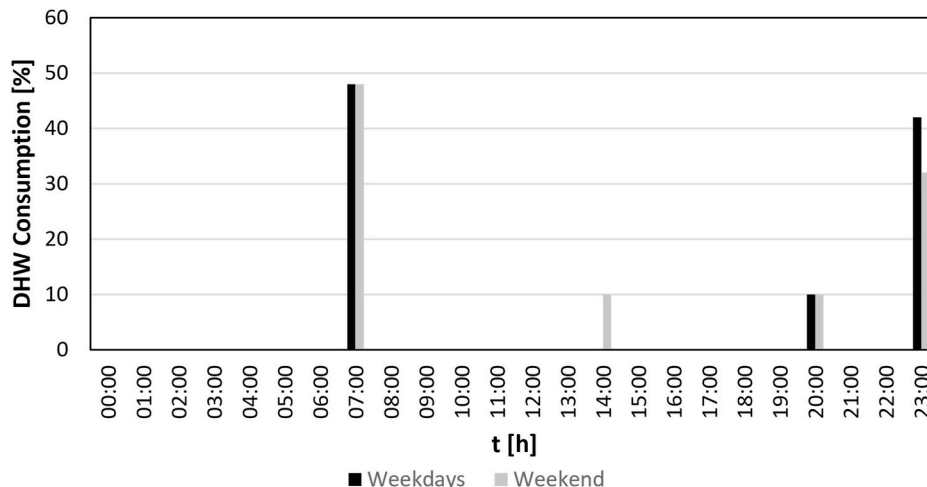


Fig. 4. Domestic Hot Water consumption profile considered.

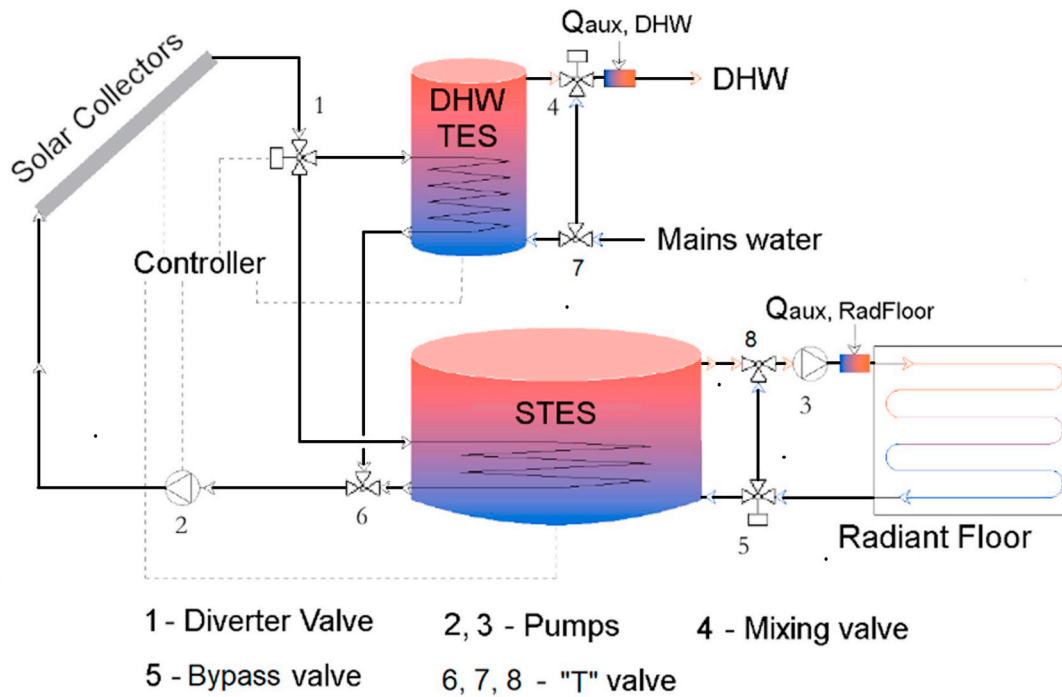


Fig. 5. Layout of the solar thermal system with DHW, seasonal storage, and underfloor heating. Priority is always given to DHW heating. When the DHW TES reservoir reaches the setpoint temperature, the surplus heat is diverted to the STES reservoir through valve 1.

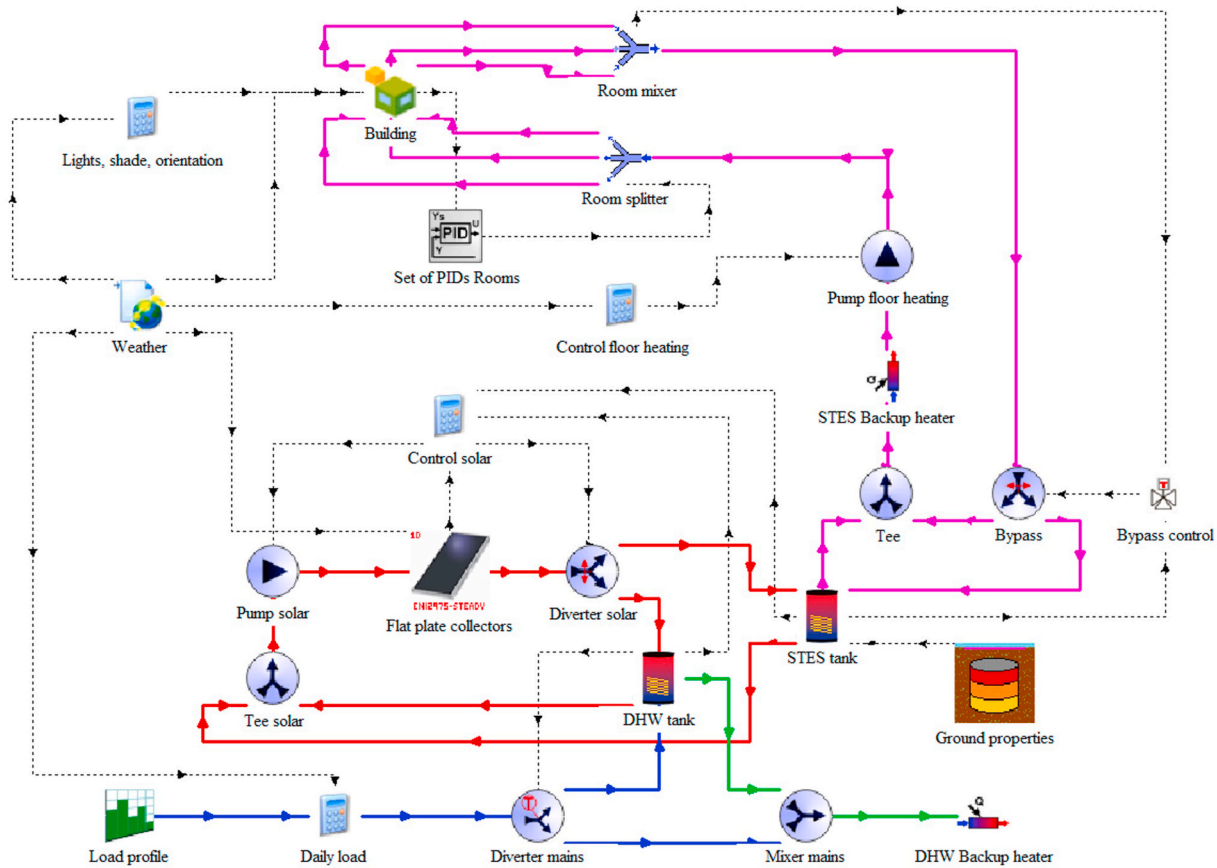


Fig. 6. TRNSYS layout of the proposed system. Red lines represent the solar energy loop, blue lines indicate the cold mains water, purple lines symbolize the underfloor heating circuit, green lines denote the DHW supply, and black dotted lines indicate control and data flow.

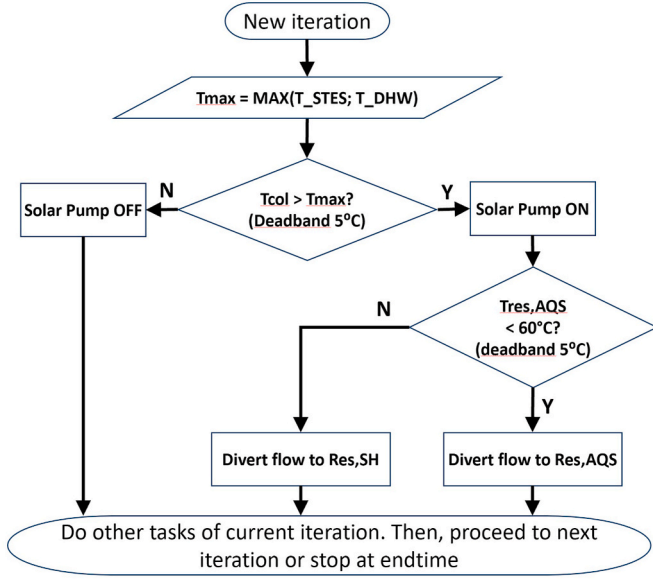


Fig. 7. Flowchart summarizing the operation of the solar thermal collector loop control.

where \dot{m}_{SH} and \dot{m}_{DHW} are the mass flow rates of warm water to the radiant floor system and of DHW water, respectively, c_w is the specific heat of liquid water, $T_{RF,in}$ and $T_{RF,out}$ are the inlet and outlet water temperatures of the radiant floor manifold, respectively, and T_{hw} and T_{cw} are the usage temperatures of DHW and water mains temperature, respectively.

The solar fractions for DHW and SH are:

$$f_{solar,DHW} = \frac{Q_{solar,DHW}}{Q_{DHW}} \quad (4)$$

$$f_{solar,SH} = \frac{Q_{solar,SH}}{Q_{SH}} \quad (5)$$

where $Q_{solar,DHW}$ represents the fraction of Q_{DHW} supplied by the solar system and $Q_{solar,SH}$ represents the fraction of Q_{SH} supplied by the solar system.

The total solar fraction is calculated as:

$$f_{solar,total} = \frac{Q_{solar,DHW} + Q_{solar,SH}}{Q_{DHW} + Q_{SH}} \quad (6)$$

The total efficiency of the solar system is calculated as:

$$\eta_{solar,total} = \frac{Q_{solar,DHW} + Q_{solar,SH}}{n_{col} \cdot A_{col} \cdot I_{solar,col}} \quad (7)$$

where n_{col} is the number of solar collectors, A_{col} is the area of one solar collector and $I_{solar,col}$ is the incident solar radiation on the collector plane per unit area.

The efficiency of the DHW and STES tanks is calculated as the ratio between the useful output heat divided by the solar thermal energy transferred to the tank:

$$\eta_{res,DHW} = \frac{Q_{solar,DHW} + Q_{solar,SH}}{Q_{col,DHW}} \quad (8)$$

$$\eta_{res,STES} = \frac{Q_{solar,SH}}{Q_{col,STES}} \quad (9)$$

where $Q_{col,DHW}$ and $Q_{col,STES}$ represent the fraction of solar energy captured by the collectors transferred to the DHW tank and STES tank, respectively.

Finally, the monthly net solar energy is a monthly energy balance considering all solar inputs and outputs, including thermal losses in the

tanks:

$$Q_{net,solar} = Q_{col,DHW} + Q_{col,STES} + Q_{solar,DHW} + Q_{solar,SH} + Q_{loss,DHW} + Q_{loss,STES} \quad (10)$$

where $Q_{loss,DHW}$ and $Q_{loss,SH}$ represent the thermal losses through the envelope of the DHW and STES reservoirs. $Q_{net,solar}$ can be positive or negative.

2.6. Methodology

First, the monthly thermal energy needs (DHW and space heating) are compared with the available solar radiation to have a general idea of the system's thermal balance evolution and the area of solar collectors required. Then, a parametric study regarding the solar collector area and the STES storage volume is performed to evaluate their impact on the system's efficiency and solar fractions, as well as the estimated system's cost. A range of 2–10 collectors and of 10 m³–50 m³ of STES tank volume are considered, given the initial size of the system and the preliminary results from Ref. [35].

Since there is no consensual optimal configuration for solar systems – we may want to have a high solar fraction, or a high system efficiency, or a compromise between the two parameters, or even the best configuration from an economic perspective – two distinct cases are selected from the parametric study for further analyses, according to the efficiency, cost, and solar fraction criteria. For both cases, the STES tank water temperature and system's efficiency evolutions are compared, as well as the energy balance (inputs vs. outputs) of the main system components (collectors, DHW tank, and STES reservoir).

In the end, the system's configuration and performance is compared with some of the most significant examples found in the literature.

3. Results and discussion

Fig. 8 presents the monthly thermal loads for DHW and SH (calculated by Eqs. (2) and (3)) and the solar radiation incident on the solar collector plane. The annual loads are about 7500 MJ for DHW and 8100 MJ for SH, while the annual solar radiation is 6300 MJ m⁻². The DHW load is nearly constant since (the house is occupied in permanence), except for a slight reduction in summer due to higher mains water temperature. Space heating is only required in the heating season (November to April), peaking in December and January. The solar radiation incident on the collectors' plane is high throughout the year, even in winter. As the figure shows, a solar system without STES could provide both DHW and SH with a high solar fraction if the collector area is large enough. Considering an average 50 % system efficiency, 16–20 m² of collectors would be required. However, this system would require a large roof area and would be extremely oversized in the summer, presenting serious installation and maintenance issues.

A parametric study was thus performed to find the best configuration. Fig. 9 shows how the total solar fraction, the global solar efficiency, and the system costs vary with the number of collectors and the STES tank volume. As expected, the solar fraction increases with both parameters, but stagnates above 5 collectors and 30 m³ of storage volume. The system efficiency decreases with more collectors (an oversized solar system is usually inefficient) and increases slightly with larger storage up to 20–30 m³, then levels off. For larger tanks, the solar energy meets all the space heating needs and extra storage is redundant.

A cost analysis was carried out with the support of a contractor in the field of building construction. The costs were estimated as 500 €/m² for the solar thermal system (including 5 solar collectors, DHW tank, pump, controller, valves, piping, and installation) and 810 €/m³ for the installation of an underground STES tank (including excavation, concrete slab, earth retaining walls, STES tank, and thermal insulation). The STES specific storage cost corresponds to about 0.63 €/kWh for 30 m³ storage (29 k€ total cost) or 0.42 €/kWh for 20 m³ storage (26 k€ total

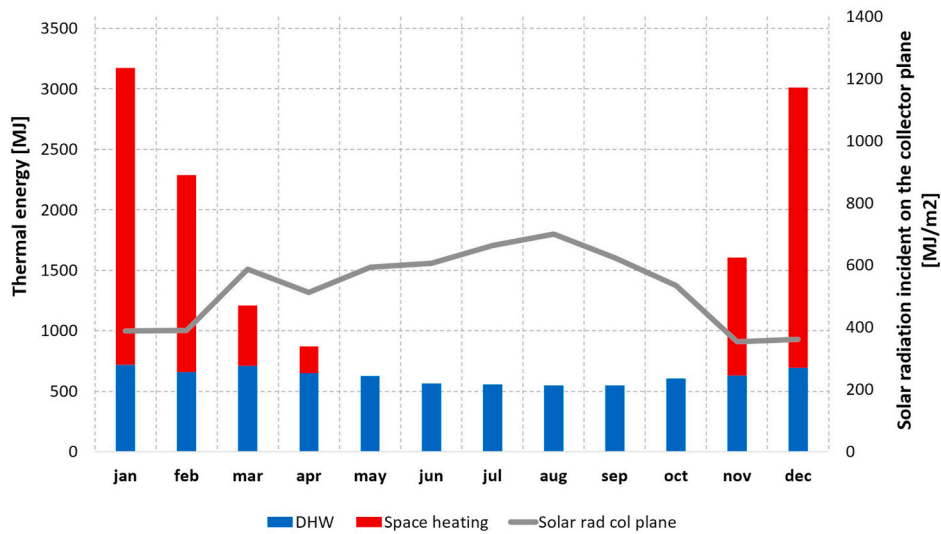


Fig. 8. Monthly thermal energy needs to produce sanitary hot water and space heating. Comparison with the solar radiation incident on the collector plane per unit area.

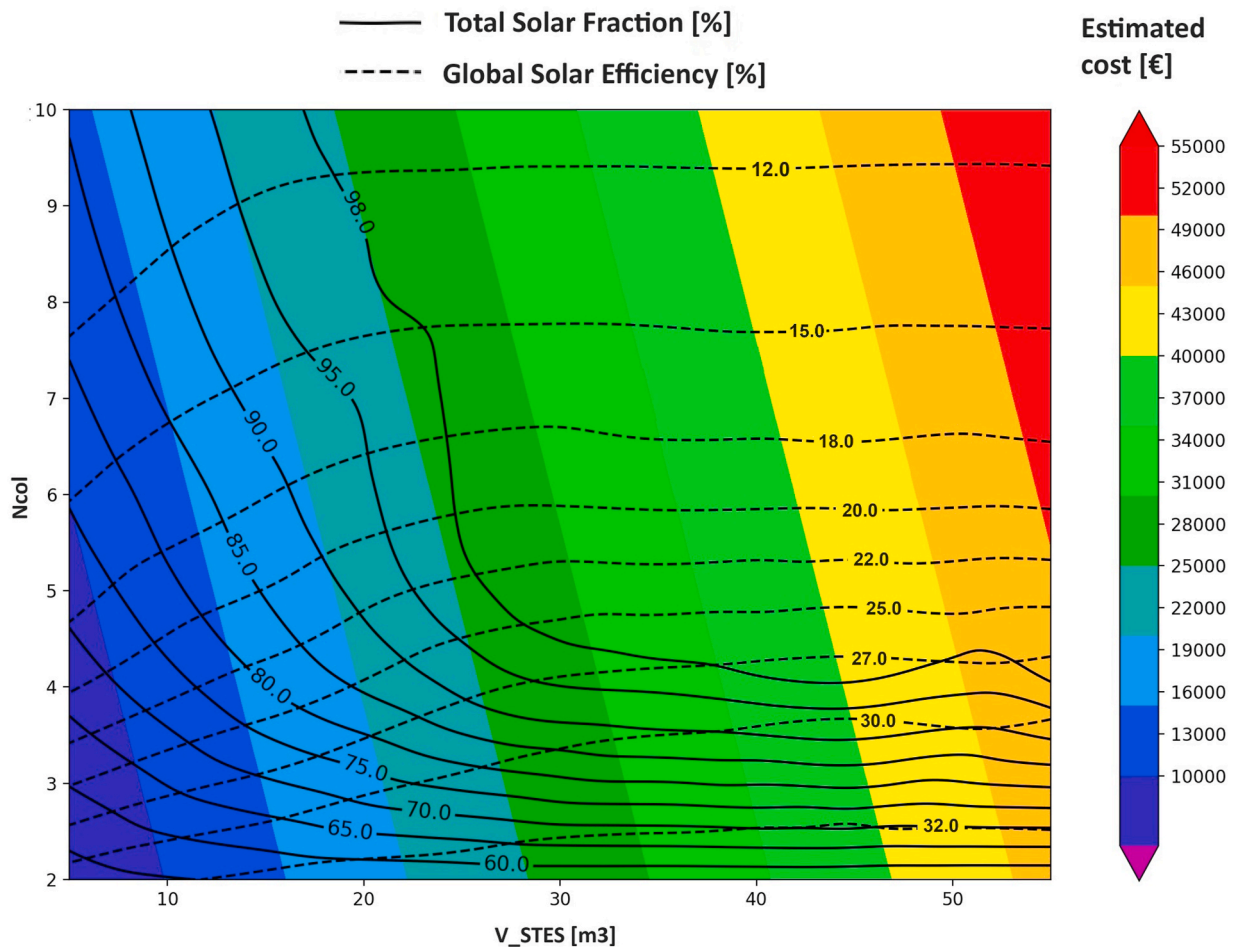


Fig. 9. – Total solar fraction (continuous lines), global system efficiency (dashed lines) and rough cost estimation as a function of the STES volume (V_{STES}) and number of solar collectors (N_{col}).

cost), considering a 20-year lifetime. Including also DHW production but excluding the cost of the radiant floor system, considering a system lifetime of 20 years, the unit cost of the thermal energy is about 0.40 €/kWh for the system with 5 collectors and 30 m³ storage, but the cost

drops to 0.35 €/kWh for the system with 10 collectors and 20 m³ storage. While it seems not yet competitive (electricity cost in Portugal is around 0.18 €/kWh), this system has an acceptable cost if funding for renewable systems is available or if the owner wants to rely solely on solar energy

for heat production. The most significant cost is the STES tank, and research is required to lower this cost and make these systems more attractive.

Fig. 10 shows the solar fraction for DHW, which depends only on the number of collectors since the system always prioritizes DHW. With 5 collectors, the solar fraction is circa 96 %, a very high value for typical thermal systems. The impact of increasing the number of collectors is minimal. Fig. 11 shows the solar fraction for space heating, which reaches 100 % with 5 collectors and 30 m³ storage. The same results can be achieved with 10 collectors and 30 m³ storage. However, increasing the number of collectors or storage volume has no effect and represents a waste of materials.

The best configuration for high solar fraction and reasonable solar efficiency comprises 5 solar collectors and a 30 m³ STES tank. The main results for this configuration are presented in Table 2. Alternatively, the same solar fractions can be achieved with 10 collectors and 20 m³ STES tank, with significantly lower costs, but only 12 % global efficiency.

The system achieves 100 % solar fraction for SH and 96 % for DHW. The storage volume for DHW could be increased to improve the solar fraction but given the probability of several consecutive cloudy days in winter, an excessively large volume would be necessary. An electrical resistance would be preferable since the amount of auxiliary power for DHW is very low. The global solar efficiency presents a relatively low value comparing to DHW only systems (40 %–60 %), and it cannot be increased without reducing the solar fraction, as shown in Fig. 9. The storage efficiency is high in both DHW and STES reservoirs, indicating adequate insulation thickness and minimal losses.

The evolution of the temperature in the STES tank is presented in Fig. 12. With 5 collectors and a 30 m³ tank, the outlet and average temperatures drop to 34 °C and 32 °C, respectively, around late February and early March. After that, there is a net positive input of heat to the STES tank, and its temperature rises to 80 °C by the end of summer. More collectors and a smaller tank lead to a faster loading rate and a higher temperature. However, the 20 m³ tank discharges faster and in February both tanks have similar temperatures. Fig. 12 also indicates that, for both cases, there is an adequate use of the storage volume, since the STES is almost completely discharged before a new charging cycle begins.

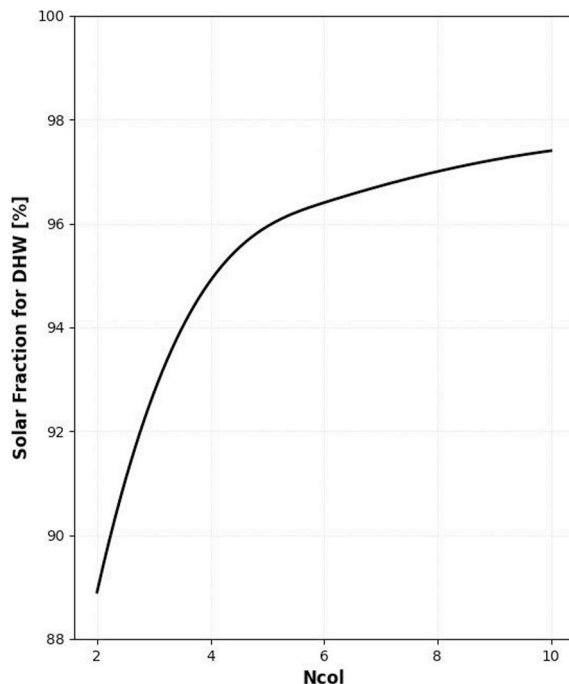


Fig. 10. Solar fraction for DHW as a function of the number of collectors.

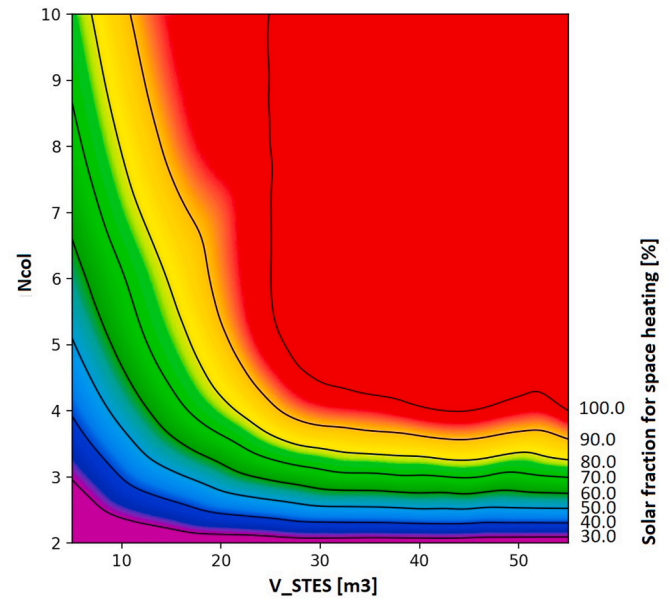


Fig. 11. Solar fraction for space heating as a function of the number of collectors and STES volume.

Table 2

Characteristics of the system for the case with a) 5 solar collectors and 30 m³ of STES storage volume, and b) 10 solar collectors and 20 m³ of STES storage volume.

	$N_{col} = 5$ $V_{STES} = 30 \text{ m}^3$	$N_{col} = 10$ $V_{STES} = 20 \text{ m}^3$
Annual heating load for DHW [MJ]	7505	7505
Annual heating load for SH [MJ]	8096	8096
Total radiation on the collector plane [MJ/m ²]	63112	63112
Solar fraction for space heating [%]	100.0	100.0
Solar fraction for DHW [%]	95.8	97.4
Total solar fraction [%]	98.0	98.7
Global solar efficiency [%]	23.2	11.7
STES storage efficiency [%]	85.5	86.8
DHW storage efficiency [%]	87.0	86.6

Fig. 13 presents the thermal energy balance of the solar collectors for both cases. The annual useful energy transfer to the tanks is similar since the loads and total solar fraction are alike. However, with 10 collectors and a 20 m³ tank, the efficiency drops significantly in summer, as more energy is available from the collectors, the smaller STES tank fills up early and the energy produced is only used to cover DHW and to compensate thermal losses.

Fig. 14 shows the thermal energy balance of the DHW system, with positive values for solar collectors ($Q_{in,resDHW}$) and backup ($Q_{aux,DHW}$) input, and negative values for losses ($Q_{loss,resDHW}$) and DHW consumption ($Q_{solar,DHW}$). The solar collectors' input is nearly constant, with minimal backup required, as is the DHW consumption. The large collector area provides enough energy, except for cloudy days in winter, when backup is required. Backup represents a very small fraction of the DHW demand. Thermal losses represent only 15 % of the input and are higher in summer, when the DHW tank is hotter. The solar fraction ranges between 87 % in February to almost 100 % from March to October.

The energy balance of the space heating system (including the STES reservoir) is represented in Fig. 15. The solar input to the STES tank ($Q_{in,resSTES}$) is always positive, indicating a heat surplus from the collectors, even in the winter peak, that is stored in the reservoir. The 30 m³ tank receives more heat from March to August, while the 20 m³ tank receives more heat from January to April, becoming fully charged before the

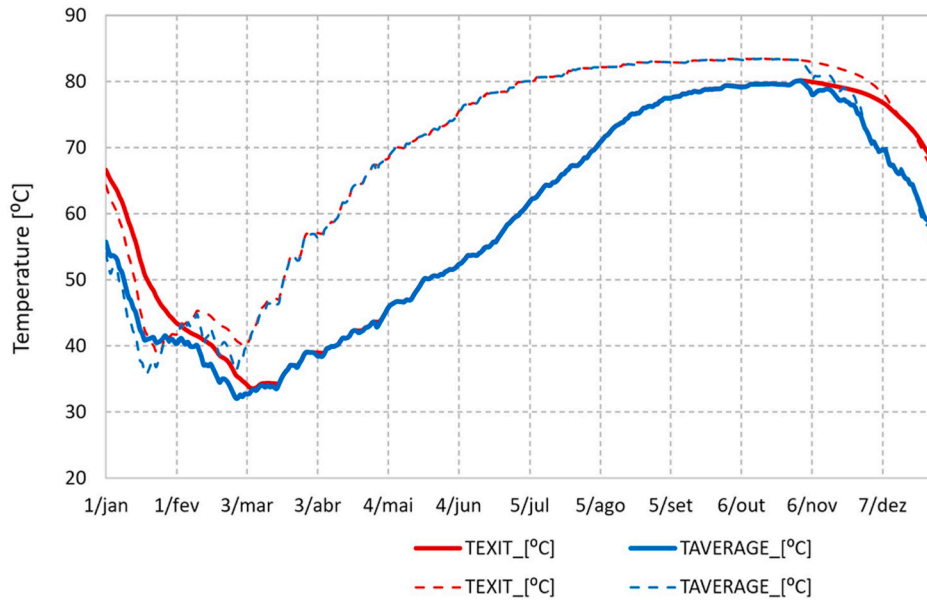


Fig. 12. Year-round temperature of the water in the STES tank for two cases: $N_{Col} = 5, V_{STES} = 30 \text{ m}^3$; and $N_{Col} = 10, V_{STES} = 20 \text{ m}^3$.

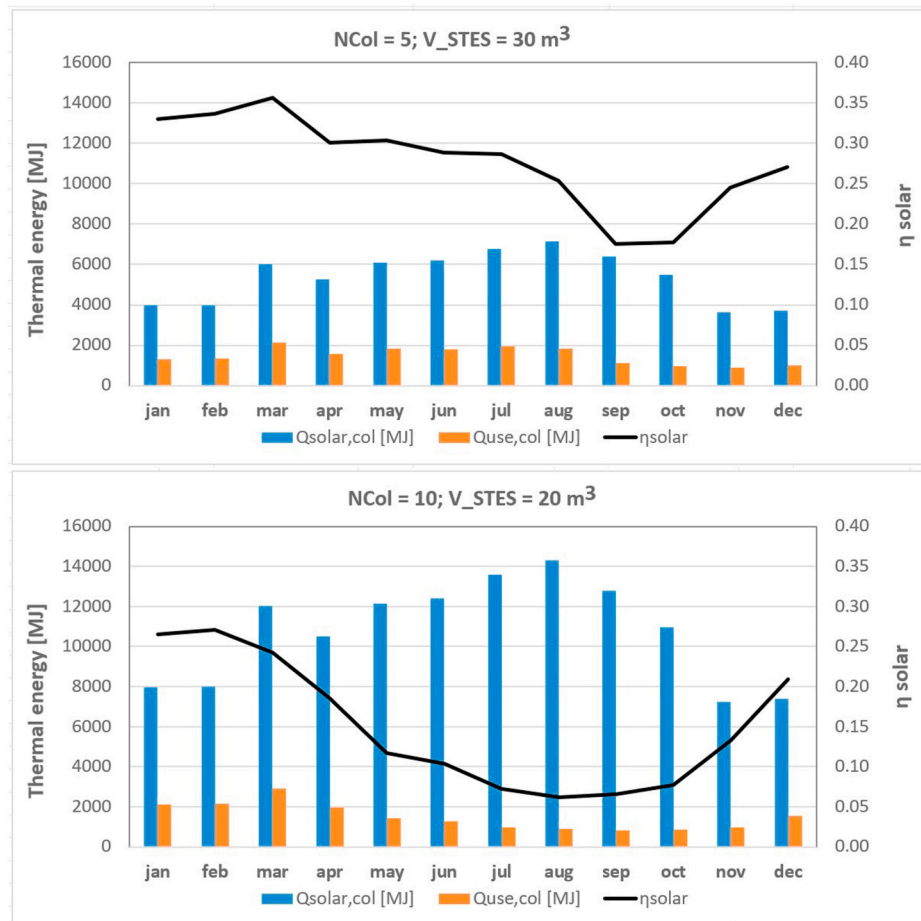


Fig. 13. Solar collectors energy balance and collector efficiency for the two selected cases.

summer peak (causing a significant waste of solar energy and a lower system efficiency). The energy consumption for space heating ($Q_{solar,SH}$) occurs only in the winter months, peaking in December and January. The thermal losses ($Q_{loss,resSTES}$) are low and similar to the DHW tank

losses, due to the thick insulation of the STES tank. The backup energy ($Q_{aux,SH}$) is negligible, resulting in a solar fraction of nearly 100 %.

Fig. 16 shows the monthly net solar energy (eq. (10)). The STES system stores excess energy from March to October, and releases it for

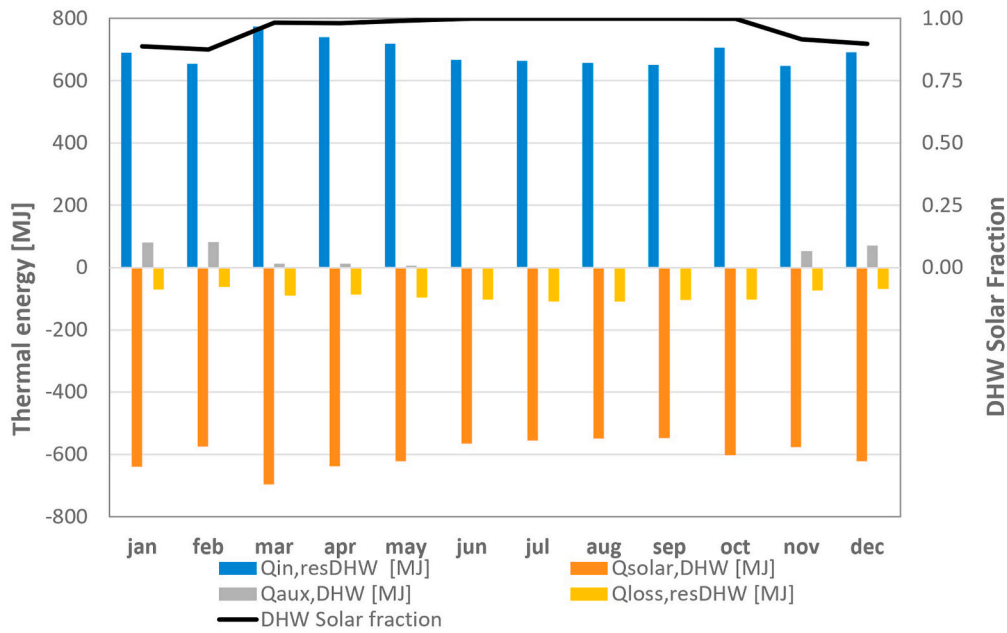


Fig. 14. DHW reservoir energy balance. Top bars represent inputs and bottom bars represent outputs.

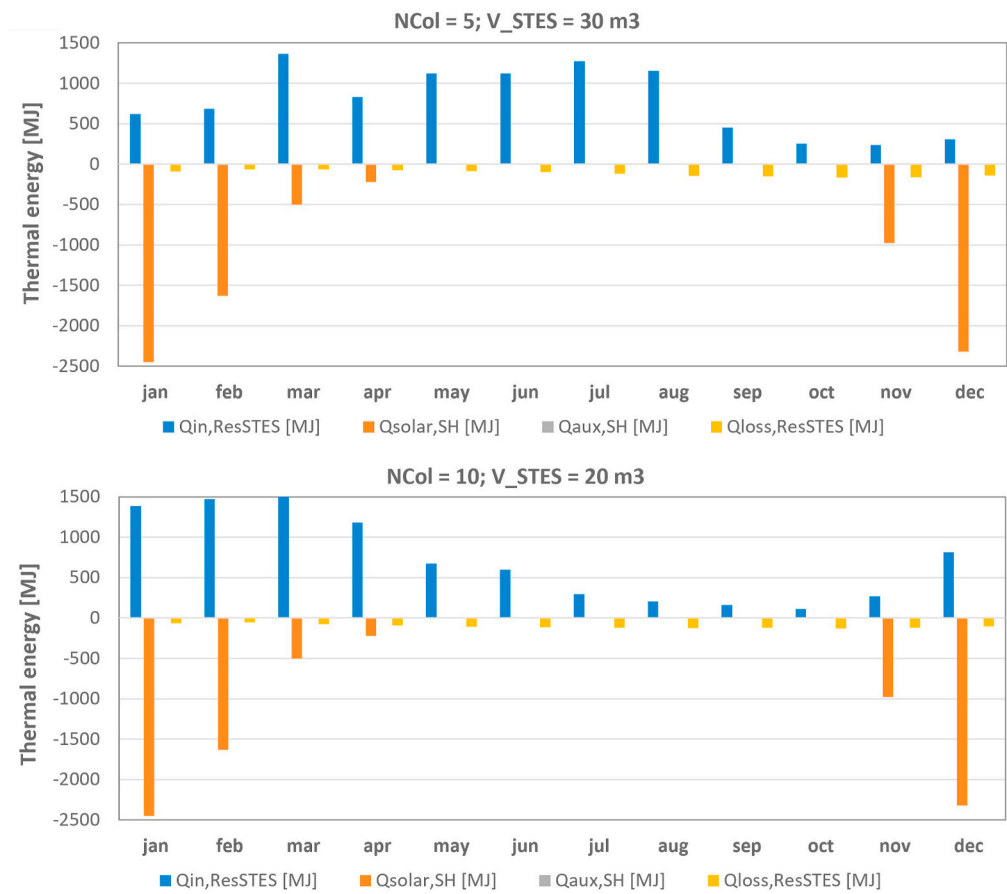


Fig. 15. STES reservoir energy balance for the two cases. Top bars represent inputs and bottom bars represent outputs.

space heating in winter, when the demand exceeds the supply. The annual energy balance is zero for the reference climate year, but it may vary for a real system: warmer years may have more input than output, and colder years may need more backup energy. Therefore, the system size should be done carefully.

Table 3 compares this simulation work with similar studies in the literature. Coimbra's climate is warmer than the other locations, with higher solar radiation and lower heating degree days (HDD). Surprisingly, SH needs are very low for Galway [16] and Ottawa [20], even considering the high thermal resistance and passive design of those

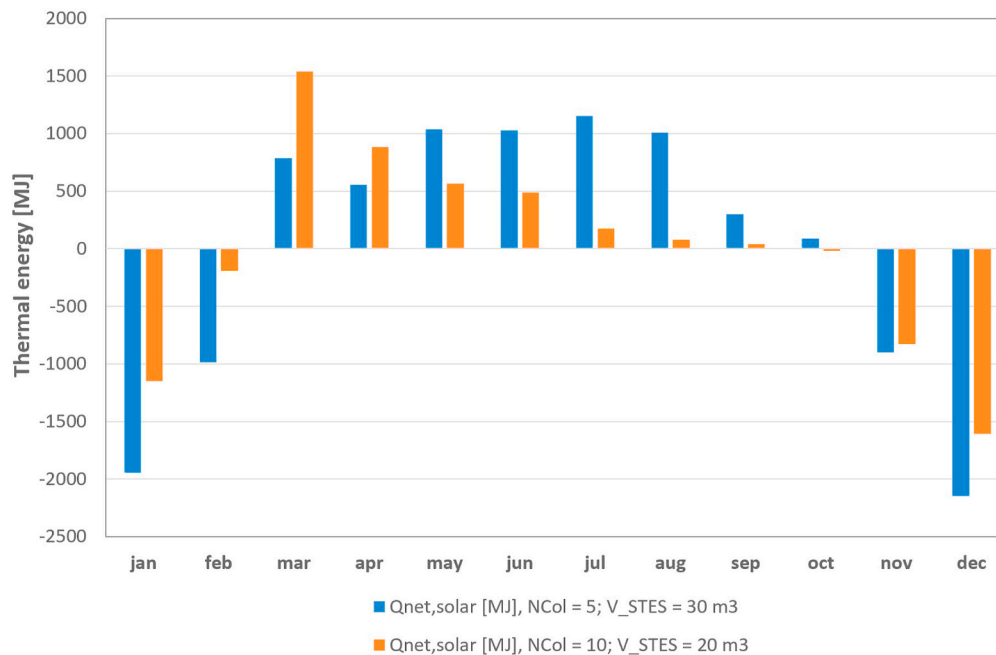


Fig. 16. Global solar energy balance for the two selected cases.

Table 3

Comparison of the simulated system with similar works.

	Residential building	Small service building	Single family house	Single family house	Single family house	Single family house
Reference	[7]	[16]	[20]	[20]	[23]	Current work
Type	Simulation	Experimental	Experimental	Simulation, improved	Simulation	Simulation
Location	Bern, Switzerland	Galway, Ireland	Ottawa, Canada	Ottawa, Canada	Thessaloniki, Greece	Coimbra, Portugal
Latitude	46.9	53.3	45.4	45.4	40.6	40.2
HDD base 18 °C (TRNSYS weather files)	3546	3017	4654	4654	1787	1255
Altitude [m]	565	25	70	70	134	50
Floor area [m ²]	924	215	150	150	120	115
Global heat transfer coef., U [W·m ⁻² ·K ⁻¹]						
- Walls	0.182	0.0989	0.21 and 0.12	0.21 and 0.12	0.35	0.402
- Ceiling	0.162	0.065	0.11	0.11	0.3	0.34
- Windows	1.00	0.9	~0.9	~0.9	2.2	2.43
Ventilation type	Not indicated	84 % heat recovery	67 % heat recovery	67 % heat recovery	Natural Ventilation	Natural Ventilation
Solar collector type	Flat plate	Evacuated tube	Evacuated tube	Evacuated tube	Flat plate	Flat plate
Solar collector tilt angle	45°	30°	60°	60°	45°	45°
Solar collector area [m ²]	187	10.6	41.6	41.6	30.0	10.5 22.0
STES volume [m ³]	180	23.0	36.3	36.3	5.0	30.0 20.0
Solar radiation on the collector plane [MJ/(m ² ·year)]	4657.0	3817.7	5923.8	5923.8	4885.4	6311.2
DWH load [MJ/(m ² ·year)]	76.3	14.3	73.5	73.5	67.6	65.3
SH load [MJ/m ² ·year]	47.1	20.1	10.8	10.8	199.6	70.4
Total load [MJ/m ² ·year]	123.4	34.3	84.3	84.3	267.2	135.7
f _{solar,DHW}	1	0.93	0.68	0.86	~1.0	0.96
f _{solar,SH}	1	0.56	0.68	1.0	0.52	1.0
f _{solar,Total}	1	0.72	0.68	0.94	0.64	0.98

buildings. SH needs are very high for Thessaloniki [23]. Notice, however, that the Galway case [16] is a service building, used only on weekdays and daytime, and possibly with high internal gains, which explains the small SH load. This work employs a smaller solar collector area than the others. However, the STES volume is larger than the Galway [16] and Thessaloniki [23] cases, but they present much lower solar fractions for SH. In general, the solar fractions for the current study are higher than all other cases. Thus, the combination of solar collector area, STES volume and solar fraction is by far more favorable in this work.

Normalizing the data by the heated area allows for better comparison. Fig. 17 plots the collector area and STES volume per heated area, and collector area/STES volume ratio. Only 3 locations have near 100 % solar fraction, but they present different geometry and U -values, making it difficult to withdraw conclusions. For Coimbra with 10 collectors and a 20 m³ tank, the ratio is about 1 m²/m³, similar to Bern and Ottawa. The collector area and STES volume increase with the climate severity, based on the HDD values. However, this trend is not clear, as the wall and windows insulation values vary for the South European climates. If Coimbra had similar U -values to Ottawa and Bern, the trend might be

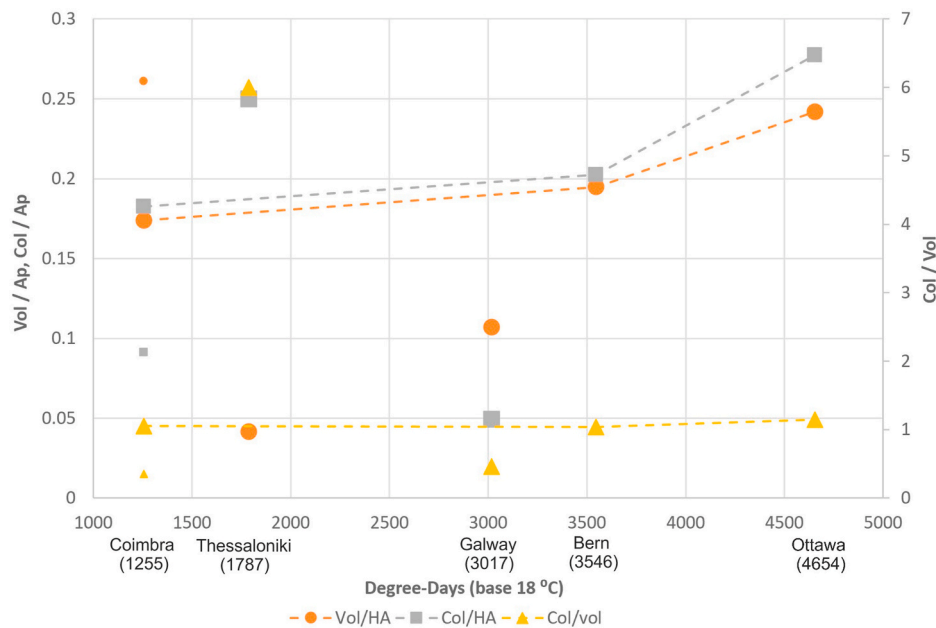


Fig. 17. Comparison of the normalized values of the collector area, STES volume and the ratio col area/STES vol. for the 5 locations. For Coimbra, the 10 collectors and 20 m³ tank case corresponds to the larger dots, and the 5 collectors and 30 m³ tank case to the smaller ones. The lines allow highlighting the 3 cases with 100 % solar fraction. HA is the Heated Floor Area.

more pronounced, as lower space heating loads would require less collector area and storage volume.

4. Conclusions

This work simulated the feasibility of using solar thermal energy to fully meet the DHW needs of a 115 m² house in the mild Southern European climate of Portugal, while making use of the surplus solar energy to also meet the space heating demand during winter, thus replacing non-renewable thermal energy sources. A conventional sensible thermal energy solar system with flat solar collectors and a DHW tank, supplemented by a STES reservoir, were used. The number of collectors and the STES tank volume were varied to face the intermittency and seasonality of solar radiation. It was concluded that 5 solar collectors (~10 m²) and a 30 m³ STES tank achieved 100 % solar fraction for space heating and 96 % for DHW, with 23 % global efficiency and a 29 k€ estimated cost. Alternatively, 10 collectors (~20 m²) and a 20 m³ tank achieved the same solar fractions with 12 % global efficiency and a 26 k€ cost. More collectors or storage were found to be unnecessary and wasteful. The system is able to present a very high solar fraction throughout the year, totally covering the SH needs with renewable energy, thus making the best use of the solar availability in summer. However, given the STES tank significant costs, this is not a competitive solution yet, thus requiring more research and/or a different type of seasonal thermal storage.

Compared to other studies, this system performed better, requiring less collector area and storage volumes per unit area. However, it would be interesting to understand how this strategy would result for buildings with different thermal insulation, space heating demands, or distinct DHW consumption profiles. Other option would be to use STES energy to also attend to DHW needs whenever possible. These adaptations are considered for future work, together with the simulation in different locations or under future weather scenarios, or the integration of latent or thermochemical storage.

Scientifically, this research contributes with novel insights by presenting a distinct case study, offering a benchmark for similar buildings and climates where comparably significant findings are lacking in the

literature. In terms of applicability, this study findings provide a basis for more effective decarbonization strategies in the building sector, by introducing renewable energy applications to mitigate carbon emissions directly.

CRediT authorship contribution statement

Gonçalo J. Brites: Writing – review & editing, Visualization, Validation, Supervision, Software, Methodology, Investigation, Conceptualization. **Manuel Garruço:** Writing – original draft, Validation, Software, Methodology, Formal analysis, Conceptualization. **Marco S. Fernandes:** Writing – review & editing, Validation. **Diogo M. Sá Pinto:** Writing – review & editing. **Adélio R. Gaspar:** Writing – review & editing, Supervision, Project administration, Funding acquisition.

Declaration of competing interest

The authors declare that they have no known competing financial interests or personal relationships that could have appeared to influence the work reported in this paper.

Acknowledgements

The presented work is framed under the research projects: ‘Adsor-Tech – Adsorption technology for supplemental thermal energy storage’, funded by the European Regional Development Fund (FEDER) through COMPETE - Operational Programme for Competitiveness and Internationalization (POCI) (ref. POCI-01-0247-FEDER-047070, Portugal 2020/ANI); ‘AdsorSeason – Long-term adsorption solar thermal energy storage’, funded by the Portuguese Foundation for Science and Technology (FCT) (ref. 2022.03339.PTDC, <https://doi.org/10.54499/2022.03339.PTDC>). This research is also sponsored by national funds through FCT, under projects ‘Associate Laboratory of Energy, Transports and Aerospace’ (ref. UIDB/50022/2020, <https://doi.org/10.54499/UIDB/50022/2020>) and ‘CLING – Climate change-based building design guidelines’ (ref. PTDC/EME-REN/3460/2021, <https://doi.org/10.54499/PTDC/EME-REN/3460/2021>). In addition, FCT funds

Marco S. Fernandes through researcher contract 2021.02975.CEECIND/CP1681/CT0002 (<https://doi.org/10.54499/2021.02975.CEECIND/CP1681/CT0002>).

References

- [1] IPCC, Summary for policymakers, in: *Climate Change 2022 - Mitigation of Climate Change*, Cambridge University Press, 2022, <https://doi.org/10.1017/9781009157926.001>.
- [2] G. Alva, Y. Lin, G. Fang, An overview of thermal energy storage systems, *Energy* 144 (2018), <https://doi.org/10.1016/j.energy.2017.12.037>.
- [3] A. Hesaraki, S. Holmberg, F. Haghighat, Seasonal thermal energy storage with heat pumps and low temperatures in building projects - a comparative review, *Renew. Sustain. Energy Rev.* 43 (2015), <https://doi.org/10.1016/j.rser.2014.12.002>.
- [4] T. Yang, W. Liu, G.J. Kramer, Q. Sun, Seasonal thermal energy storage: a techno-economic literature review, *Renew. Sustain. Energy Rev.* 139 (2021), <https://doi.org/10.1016/j.rser.2021.110732>.
- [5] J. Xu, R.Z. Wang, Y. Li, A review of available technologies for seasonal thermal energy storage, *Sol. Energy* 103 (2014), <https://doi.org/10.1016/j.solener.2013.06.006>.
- [6] P. Pinel, C.A. Cruickshank, I. Beausoleil-Morrison, A. Wills, A review of available methods for seasonal storage of solar thermal energy in residential applications, *Renew. Sustain. Energy Rev.* 15 (7) (2011), <https://doi.org/10.1016/j.rser.2011.04.013>.
- [7] W. Villasmil, M. Troxler, R. Hendry, P. Schuetz, J. Worlitschek, Control strategies of solar heating systems coupled with seasonal thermal energy storage in self-sufficient buildings, *J. Energy Storage* 42 (Oct. 2021) 103069, <https://doi.org/10.1016/j.est.2023.106685>.
- [8] M. Ryland, W. He, Domestic thermal energy storage applications: what parameters should they focus on? *J. Energy Storage* 60 (Apr) (2023) <https://doi.org/10.1016/j.est.2023.106685>.
- [9] M.S. Fernandes, G.J.V.N. Brites, J.J. Costa, A.R. Gaspar, V.A.F. Costa, A thermal energy storage system provided with an adsorption module – dynamic modeling and viability study, *Energy Convers. Manag.* 126 (Oct. 2016) 548–560, <https://doi.org/10.1016/j.enconman.2016.08.032>.
- [10] M.S. Fernandes, G.J.V.N. Brites, J.J. Costa, A.R. Gaspar, V.A.F. Costa, Modeling and parametric analysis of an adsorber unit for thermal energy storage, *Energy* 102 (May 2016) 83–94, <https://doi.org/10.1016/j.energy.2016.02.014>.
- [11] R.G. Raluy, S. Guillén-Lambea, L.M. Serra, M. Guadalfajara, M.A. Lozano, Environmental assessment of central solar heating plants with seasonal storage located in Spain, *J. Clean. Prod.* 314 (2021), <https://doi.org/10.1016/j.jclepro.2021.128078>.
- [12] S. Chu, S. Sethuvenkatraman, M. Goldsworthy, G. Yuan, Techno-economic assessment of solar assisted precinct level heating systems with seasonal heat storage for Australian cities, *Renew. Energy* 201 (Dec. 2022) 841–853, <https://doi.org/10.1016/j.renene.2022.11.011>.
- [13] A. Lyden, C.S. Brown, I. Kolo, G. Falcone, D. Friedrich, Seasonal thermal energy storage in smart energy systems: district-level applications and modelling approaches, *Renew. Sustain. Energy Rev.* 167 (Oct. 2022) 112760, <https://doi.org/10.1016/j.rser.2022.112760>.
- [14] F. Ochs, W. Heidemann, H. Müller-Steinhagen, Performance of Large-scale seasonal thermal energy stores, *J. Solar Energy Eng. Transact. ASME* 131 (4) (2009), <https://doi.org/10.1115/1.3197842>.
- [15] J.A. Kroll, F. Ziegler, The use of ground heat storages and evacuated tube solar collectors for meeting the annual heating demand of family-sized houses, *Sol. Energy* 85 (11) (Nov. 2011) 2611–2621, <https://doi.org/10.1016/j.solener.2011.08.001>.
- [16] J. Clarke, S. Colclough, P. Griffiths, J.T. McLeskey, A passive house with seasonal solar energy store: in situ data and numerical modelling, *Int. J. Ambient Energy* 35 (1) (2014), <https://doi.org/10.1080/01430750.2012.759153>.
- [17] S. Colclough, T. McGrath, Net energy analysis of a solar combi system with Seasonal Thermal Energy Store, *Appl. Energy* 147 (2015), <https://doi.org/10.1016/j.apenergy.2015.02.088>.
- [18] I. Beausoleil-Morrison, B. Kemery, A.D. Wills, C. Meister, Design and simulated performance of a solar-thermal system employing seasonal storage for providing the majority of space heating and domestic hot water heating needs to a single-family house in a cold climate, *Sol. Energy* 191 (2019), <https://doi.org/10.1016/j.solener.2019.08.034>.
- [19] M. Pinamonti, I. Beausoleil-Morrison, A. Prada, P. Baggio, Water-to-water heat pump integration in a solar seasonal storage system for space heating and domestic hot water production of a single-family house in a cold climate, *Sol. Energy* 213 (2021), <https://doi.org/10.1016/j.solener.2020.11.052>.
- [20] C. Meister, I. Beausoleil-Morrison, Experimental and modelled performance of a building-scale solar thermal system with seasonal storage water tank, *Sol. Energy* 222 (2021), <https://doi.org/10.1016/j.solener.2021.05.025>.
- [21] Z. Ma, H. Bao, A.P. Roskilly, Feasibility study of seasonal solar thermal energy storage in domestic dwellings in the UK, *Sol. Energy* 162 (Mar. 2018) 489–499, <https://doi.org/10.1016/j.solener.2018.01.013>.
- [22] Z. Ma, H. Bao, A.P. Roskilly, Seasonal solar thermal energy storage using thermochemical sorption in domestic dwellings in the UK, *Energy* 166 (2019), <https://doi.org/10.1016/j.energy.2018.10.066>.
- [23] C.N. Antoniadis, G. Martinopoulos, Simulation of solar thermal systems with seasonal storage operation for residential scale applications, *Procedia Environ Sci* 38 (2017), <https://doi.org/10.1016/j.proenv.2017.03.124>.
- [24] C.N. Antoniadis, G. Martinopoulos, Optimization of a building integrated solar thermal system with seasonal storage using TRNSYS, *Renew. Energy* (2019), <https://doi.org/10.1016/j.renene.2018.03.074>.
- [25] G. Englmaier, W. Kong, J. Brinkø Berg, S. Furbo, J. Fan, Demonstration of a solar combi-system utilizing stable supercooling of sodium acetate trihydrate for heat storage, *Appl. Therm. Eng.* 166 (2020), <https://doi.org/10.1016/j.applthermaleng.2019.114647>.
- [26] H.H. Öztürk, Experimental evaluation of energy and exergy efficiency of a seasonal latent heat storage system for greenhouse heating, *Energy Convers. Manag.* 46 (9–10) (2005), <https://doi.org/10.1016/j.enconman.2004.07.001>.
- [27] R. Köll, et al., An experimental investigation of a realistic-scale seasonal solar adsorption storage system for buildings, *Sol. Energy* 155 (2017), <https://doi.org/10.1016/j.solener.2017.06.043>.
- [28] J.P. Gouveia, P. Palma, Energy efficiency of the housing stock in Portugal [Online]. Available: <https://www.eppedia.eu/article/energy-efficiency-housing-stock-portugal>, 2021.
- [29] International Energy Agency, Portugal 2021 - energy policy review [Online]. Available: <https://www.iea.org/reports/portugal-2021>, 2021.
- [30] H. Ritchie, M. Roser, P. Rosado, Portugal: energy country profile [Online]. Available: <https://ourworldindata.org/energy/country/portugal>, 2022.
- [31] DGE - Directorate General for Energy and Geology, Assessment of District Heating and Cooling Potential in Portugal, DEIR Studies on the Portuguese Energy System 003', 2021 [Online]. Available: <https://www.dgeg.gov.pt/media/t2bngb4c/district-heating-and-cooling-potential-in-portugal-deir-studies-003-2021.pdf>.
- [32] M. Kotteck, J. Grieser, C. Beck, B. Rudolf, F. Rubel, World Map of the Köppen-Geiger climate classification updated, *Meteorol. Z.* 15 (3) (Jul. 2006) 259–263, <https://doi.org/10.1127/0941-2948/2006/0130>.
- [33] PORDATA, Electricity consumption per inhabitant: total and by type of consumption [Online]. Available: <https://www.pordata.pt/en/Municipalities/Electricity+consumption+per+inhabitant+total+and+by+type+of+consumption-435>. (Accessed 1 May 2022).
- [34] INE - Instituto Nacional de Estatística (Statistics Portugal) and DGE - Directorate General for Energy and Geology, 'Survey on energy consumption in the domestic sector - 2020 [in Portuguese]', <https://www.ine.pt/xurl/pub/48433981>, 2021.
- [35] M. Garruço, 'Solar Thermal System with Seasonal Storage, Faculty of Sciences and Technology of the University of Coimbra, 2022 [in Portuguese]'.